Targeting Breast Cancer with N-Acetyl-D-Glucosamine: Integrating Machine Learning and Cellular Assays for Promising Results

Ömür Baysal
omurbaysal@mu.edu.tr
Muğla Sıtkı Koçman University
Deniz Genç
Muğla Sıtkı Koçman University
Ragıp SOner Silme
Istanbul University
Kevser Kübra Kırboğa
Bilecik Seyh Edebali University
Dilek Çoban
Muğla Sıtkı Koçman University
Naeem Abdul Ghafoor
Muğla Sıtkı Koçman University
Leyla Tekin
Muğla Sıtkı Koçman University
Osman Bulut
Muğla Sıtkı Koçman University

Research Article

Keywords: anti-tumor agent, apoptosis, breast cancer, Fas expression, machine learning, N-acetyl-D-glucosamine

Posted Date: June 26th, 2023

DOI: https://doi.org/10.21203/rs.3.rs-3063549/v1

Additional Declarations: No competing interests reported.

Version of Record: A version of this preprint was published at Anti-Cancer Agents in Medicinal Chemistry on March 1st, 2024. See the published version at https://doi.org/10.2174/0118715206270568231129054853.

Abstract

Early diagnosis of breast cancer can reduce prognosis and mortality rates, but alternative treatments are needed. We studied the effect of N-acetyl-D-glucosamine (D-GlcNAc) on breast cancer using machine learning and cell assays. MCF-7 and 4T1 cell lines (ATCC) were cultured in the presence and absence of varying concentrations of D-GlcNAc (0.5 mM, 1 mM, 2 mM, and 4 mM) for 72 hours. A xenograft mouse model for breast cancer was established by injecting 4T1 cells into mammary glands. D-GlcNAc (2 mM) was administered intraperitoneally to mice daily for 28 days, and histopathological effects were evaluated at pre-tumoral and post-tumoral stages. Treatment with 2 mM and 4 mM D-GlcNAc significantly decreased cell proliferation rates in MCF-7 and 4T1 cell lines and increased Fas expression. The number of apoptotic cells was significantly higher than in untreated cell cultures ($P < 0.01$ - $P < 0.0001$). D-GlcNAc administration also considerably reduced tumour size, mitosis, and angiogenesis in the post-treatment group compared to the control breast cancer group ($P < 0.01$ - $P < 0.0001$). Molecular docking/dynamic analysis revealed a high binding affinity of D-GlcNAc to the marker protein HER2, which is involved in tumor progression and cell signalling. Our study demonstrates the positive effect of D-GlcNAc administration on breast cancer cells, leading to increased apoptosis and Fas expression in the malignant phenotype. The binding affinity of D-GlcNAc to HER2 suggests a potential mechanism of action. These findings contribute to understanding D-GlcNAc as a potential anti-tumor agent for breast cancer treatment.

1. Introduction

Breast cancer is among the most common cancers with a high mortality rate in women [1]. Current treatments include surgery followed by chemotherapy or radiotherapy, or in some cases, hormone or targeted therapies [2]. However, the mortality rate is still high due to delayed diagnosis [3]. Therefore, developing pre-and post-cancer treatment options is crucial to reduce breast cancer's prognosis and mortality rates.

N-acetyl-d-glucosamine (D-GlcNAc) is an amino sugar, replacing a hydroxyl group with an amine group [4]. D-GlcNAc and its derivatives have many biological activities, including antimicrobial, anti-tumor, and immunity-enhancer properties [4–6]. Glycosylation-cancer interaction attracts the attention of researchers. In a previous study, GlcNAc has shown a modulator effect on Tumor necrosis factor (TNF)-related apoptosis-inducing ligand (TRAIL) on non-small cell lung [4]. Correspondingly, the findings on the increased size of tumor cell glycopeptides have been partly associated with the increase in β1–6 branching of N-glycans, resulting from enhanced expression of N-acetylglucosaminyltransferase V (GnT-V, MGAT5). Increased transcription of the MGAT5 gene induced by various oncogenic transcription factors such as viral- and chemical-induced carcinogenesis has been acknowledged [7]. Altered protein glycosylation has correlated well with tumorigenesis, but its role remains unclear [8].

Our previous studies showed the possible binding effect of D-GlcNAc on the proteins in the pathogenicity of SARS-CoV-2, considering the binding region peculiar to asparagine rich regions [9, 10]. From that point,

we have assumed the function and inhibitory role of D-GlcNAc on striking cell reduction in the growth and metastasis of mammary tumours induced by a viral oncogene. The viral agents involving bovine leukemia virus [11, 12], human mammary tumor virus [13], human papillomavirus [14], Epstein–Barr virus (EBV) [15–17], and human cytomegalovirus (HCMV) [18–21] have been associated with breast cancer. Still, their role in breast cancer remains not well understood [22, 23].

The importance of HER2 activity inhibition methods in cancer studies also attracts the attention of researchers. HER2, a ligand-free tyrosine kinase receptor of the HER family, is frequently overexpressed in breast cancer due to its protooncogene property. As known, HER2 suppresses apoptosis to enhance cell survival causing uncontrolled proliferation and tumor growth [24]. Therefore, suppressing with a compound which shows affinity on the surface and inactivation of HER2 could inhibit uncontrolled proliferation and leads to apoptosis.

In our present study, we aimed to investigate the apoptotic effect, induction of Fas expression and a decrease in the proliferation with D-GlcNAc at various concentrations determined by the machine learning method on the MCF-7 and 4T1 breast cancer cell lines considering the suppressive effect on the breast cancer murine model. Furthermore, the binding affinity of D-GlcNAc on HER2 was investigated by a computational biology approach involving molecular docking and dynamics analysis to confirm our assumed D-GlcNAc's mode of action.

2. Materials and Methods

2.1. Preliminary assessment of D-GlcNAc potency against breast cancer cell line

To assess the D-GlcNAc potency, several machine learning models were developed to predict the EC_{50} (the dose effective at producing 50% maximal response) of D-GlcNAc against the MCF-7 cell lines. The bioactivity data for all compounds with known EC_{50} values against MCF-7 cell line derived from functional cell-based assays reported in the scientific literature was curated from the ChEMBL database [25]. The dataset was limited to compounds with molecular weight between 200–700 g/mol and ALogP (Log of partition coefficient, a measurement of compounds' lipophilicity). Molecule ChEMBL IDs between 1 and 6, the dataset was conducted as non-redundant and the EC_{50} values were converted into pEC_{50} via -Log (EC_{50}) transformation. The non-redundant curated dataset is provided in Supplementary Materials S1.

To utilize the curated dataset in building a machine learning model, the different sets of features/descriptors were calculated from each compound from their respective canonical SMILES (Simplified Molecular-Input Line-Entry System, a notation to represent chemical structures as 1D-arrays). The set of features utilized in this study involves M2V (Mol2vec), PCH (PubChem fingerprints), MOR (Morgan fingerprints), and RDP (RDKit properties). M2V descriptors were calculated via the *mol2vec* library (v0.1), PCH and descriptors were calculated via the *DeepPurpose* library (v0.1.5), and RDP and

MOR descriptors were calculated via the *rdkit-pypi* library (v2022.3.4) [26–28]. To identify which machine learning algorithm would perform the best with each set of descriptors, five machine learning algorithms available within the *Scikit-learn* (v0.2.9) library, namely, LGBR (Light Gradient Boosting Regressor), EGBR (Extreme Gradient Boosting Regressor), SVR (epsilon-Support Vector Regressor), RFR (Random Forest Regressor), and KNR (K Neighbors Regressor) algorithms screened were used with each set of descriptors [29]. The *SelectKBest* module with *f_regression* scoring function within the *Scikit-learn* library was utilized as a feature selection criterion to select the top ranking 20%, 40%, 60%, and 80% of the descriptors that correlated with the dependent variable (i.e., the pEC_{50} values). In total, 4 sets of descriptors with 4 different fractions were used with five machine-learning algorithms to generate machine-learning models.

Each model was evaluated via 5-fold cross-validation (i.e., in each instance, 80% of the dataset was used to train the model, and the remaining 20% was used to evaluate the model's performance). The performance of each model was also evaluated based on the average of their R^2 (Coefficient of determination), RMSE (Root Mean Squared Error), MSE (Mean Squared Error), and MAE (Mean Absolute Error) following the 5-fold cross-validation. The model with the best performance metrics on the testing dataset was selected to predict the EC_{50} of D-GlcNAc. All computational steps were performed in Python 3.8 environment.

2.2. Cell lines

The MCF-7 breast cancer cells (HTB-22) and 4T1 mammary carcinoma cells (CRL-2539) were obtained from ATCC Company (Manassas, VA, US). MCF-7 and 4T1 cell lines were separately cultured in Dulbecco's Modified Eagle Medium (DMEM) (Gibco, MA, US) supplemented with 5% Fetal Bovine Serum (FBS) (Sigma-Aldrich, MO, US) and 1% penicillin/streptomycin (Thermo Fisher Scientific, MA, US) in a 95% humidified and 5% CO_2 chamber until reaching 90% confluence. Cells were treated with 0.25% trypsin EDTA solution before using for cultures.

2.3. Culture conditions

The culture conditions were performed as Liang et al.4 described with some modifications. In brief, MCF-7 or 4T1 cells were seeded in 48-well culture plates at an optimal density (10^4 cells/well) in DMEM supplemented with 5% FBS and 1% penicillin/streptomycin with or without D-GlcNAc (0.5 mM, 1 mM, 2 mM, and 4 mM) in a 5% CO_2 incubator at 37°C for 72 hours. Cultures were repeated six times for each well.

2.4. Annexin V/7-AAD staining

The cultured cells were stained with phycoerythrin labelled Annexin V/7-AAD (7-aminoactinomycine-D) according to the manufacturer's instructions (Annexin V/7-AAD kit, BD Biosciences, US). The cell pellet was washed and resuspended in 100 µL binding buffer at a concentration of 10^5-10^6 cells/mL; 5 µL of Annexin V together with 5 µL 7-AAD was added to 100 µL cell suspension. MCF-7 cells were incubated for 15 minutes in the dark [30]. The samples were analyzed by flow cytometry (BD Accuri C6 Plus, US), and

data were recorded as the percentage of the cells in four quadrants as follows; Top-right: Late apoptosis, Top-left: Necrosis, Bottom-right: early apoptosis, Bottom-left: Living cells.

2.5. Fas analysis

The cultured MCF-7 or 4T1 cells were stained with anti-human-CD95 (Fas) FITC or anti-mouse-CD95 FITC, according to the manufacturer's instructions (BD Biosciences, US). The cell pellet was washed and resuspended in 100 µL binding buffer at a concentration of 10^5-10^6 cells/mL; 5 µL of anti-CD95 was added to 100 µL cell suspension. The cells were incubated for 15 minutes in the dark. The samples were analyzed by flow cytometry (BD Accuri C6 Plus, US), and data were recorded as the mean fluorescence intensity (MFI).

2.6. Proliferation analysis

MCF-7 or 4T1 cells (10^6 cells/mL) were labelled with 1 µM Carboxyfluorescein succinimidyl ester (CFSE) (Thermofisher, US) prior to culture as described by Matera et al. [31]. The cultured cells were analyzed via flow cytometry in the n FL-1 channel to determine the proliferation rate. The data was recorded as the mean fluorescence intensity (MFI).

2.7. Breast cancer animal model and treatment

The xenograft mouse model for breast cancer was performed as previously described by Pulaski and Ostrand-Rosenberg [32]. The ethical approval was obtained from the Muğla Sıtkı Koçman University Experimental Animal Center. All experiments were conducted following the United Kingdom Animals (Scientific Procedures) Act (1986) and the Muğla Sıtkı Koçman University ethical guidelines. The sample size was determined with G-power analysis. The total sample size was calculated as twenty-four animals when the effect size was 0.75, type I error was 0.05, and power was 0.80 for four groups. 4T1 mammary carcinoma cells ($1x10^6$) were suspended in 50 µL of Phosphate Buffer Solution (PBS) and injected into the mammary gland of 6-8-week-old female BALB/c mice. After injection, mice were monitored for tumor onset daily by palpating the injection area with the index finger and thumb for the presence of a tumor. Tumor diameter reached 14–16 mm at 14–18 days after injection of 4T1 cells. Mice were treated with a daily injection of D-GlcNAc (2 mM) on the 1st day or 18th day after inoculation of 4T1 cells to evaluate the pre-tumoral or post-tumoral effect of D-GlcNAc, for 28 days. Groups were determined as follows: 1) Group 1: Control Group (n = 6), 2) Group 2: Breast Cancer Group (n = 6), 3) Group 3: D-GlcNAc pre-treatment group (n = 6), 4) Group 4: D-GlcNAc post-treatment group (n = 6). Animals were sacrificed on the 56th day of the experimental protocol.

2.8. Histopathological analysis

The left breast tissues were excised, fixed with 10% formalin, and paraffin-embedded. For histopathological examination, 4-µm sections of formalin-fixed paraffin-embedded breast tissues were cut, placed on glass slides, deparaffinized with xylene, and rehydrated in 30–100% ethanol. Sections were stained with haematoxylin and eosin for histopathological examination [33].

2.9. Molecular docking and dynamics analysis

The 3D structure for the human epidermal growth factor receptor 2 (HER2, PDB ID: 3WSQ) was retrieved from the RCSB database, and the 3D structure of D-GlcNAc (CID: 439174) was downloaded from PubChem. The protein structure files were stripped from all heteroatoms, Gasteiger charges were applied, and polar hydrogens were added via AutoDock (v1.5.7) [34]. Blind molecular docking was performed for HER2 against D-GlcNAc via AutoDock Vina (v1.2.1) to identify potential affinity between the receptor- D-GlcNAc pairs [35]. Further details on the configurations used for the molecular docking analysis are given in Supplementary Materials S2. The results were also confirmed by the SwissDock server [36].

Molecular Dynamics analysis was performed between the top pose of the receptor- D-GlcNAc pairs using Nanoscale Molecular Dynamics (NAMD, v2.14) [37]. The CHARMM36m forcefield was used to parametrize the receptors and D-GlcNAc, and the simulation system was optimized to simulate the cell microenvironment [38, 39]. The receptors with top docked pose to D-GlcNAc were submerged in a rectangular box with TIP3P water, neutralized KCl and the final concentration of KCl and NaCl was maintained at 0.15 M; the simulation was performed for 1 ns under the NVT ensemble with the backbone atoms restrained, followed by 50 ns simulation under NPT ensemble with no restrains in the system. All molecular dynamic simulations were carried out on 310.15 K and performed in duplicates. The molecular dynamics' trajectory was analyzed via MDAnalysis (v2.0.0) [40]. The configuration file to replicate the molecular dynamics simulations are provided in Supplementary Materials S3.

2.10. Statistical analysis

Differences between the groups were analyzed using the GraphPad Prism 9.0 version (GraphPad Software, Inc., CA, US). Data were given as mean (Mean) ± standard deviation (SD) (minimum-maximum) values in each group. In detail, the secreted cytokine levels were in pg/mL and given as mean ± SD. Flow cytometry analysis for cytokine-secreting cells and B lymphocyte subsets were presented as percentages (%) of cell populations. Graphical presentation and statistical analysis were calculated using GraphPad Prism 8 software (Graphpad Software Inc., US). Comparison of the data with more than two groups was done by one-way ANOVA test. The Mann-Whitney U test analyzed histopathological data. An unpaired Student's t-test was used to compare cytokine levels between groups. $P < 0.05$ values were considered statistically significant, and $P < 0.01$-$P < 0.0001$ values were also considered highly significant.

3. Results

3.1. Preliminary assessment of D-GlcNAc potency against breast cancer cell line

In total, 708 compounds with known EC_{50} against the MCF-7 cell line were curated (Supplementary Materials S1), and the evaluation metrics for the top 5 machine learning models (based on the average R^2 from cross-validated test set) developed in this study are provided in **Table 1**, the benchmarks for all models are provided in Supplementary Material S4. The SVR/NuSVR algorithm produced the best results with MOR descriptors (without any feature selection). The best-performing model was based on the SVR

algorithm. The top performing SVR model with MOR descriptors (represented as 1024-Bit vectors) 0.899 and 0.763 R^2 after 10-fold cross-validation on the train and test sets were obtained, respectively. The latter model's MSE, RMSE, and MAE on the train and test sets after 10-fold cross-validation were 0.341, 0.583, 0.335 and 0.752, 0.855, 0.610, respectively. Further details and codes to reproduce the model and its evaluation metrics are provided in Supplementary Materials S5.

The canonical SMILES for D-GlcNAc is "CC(=O)NC1C(C(C(OC1O)CO)O)O" (PubChem CID: 439174), the predicted pEC_{50} for D-GlcNAc via the top performing machine learning model developed in this study was 5.760, which translated into 3.151 mM. This prediction further set the basis for the hypothesis to investigate D-GlcNAc activity against MCF7 cell lines *in vitro* and subsequently *in vivo*.

Table 1. Evaluation metrics for the top performing ten machine learning models.

Machine learning algorithm	Descriptor set	R^2	MSE	RMSE	MAE
SVR	MOR (1024)	0.775	0.726	0.845	0.599
NuSVR	MOR (1024)	0.771	0.740	0.853	0.615
SVR	MOR (512)	0.769	0.749	0.858	0.609
NuSVR	MOR (512)	0.764	0.765	0.868	0.626
HGBM	MOR (1024)	0.758	0.745	0.845	0.581
*R^2, MSE, RMSE, and MAE provided are the mean of the predictions on the test sets following 5-fold cross-validation					

3.2. D-GlcNAc decreased the proliferation rate and increased Fas expression of MCF-7 and 4T1 cells

The proliferation rate significantly decreased with 2 mM and 4 mM D-GlcNAc administration in MCF-7 and 4T1 cell lines compared with untreated cell cultures (*P <0.01-P <0.0001*) (**Figure 1**). Fas expression significantly increased with 1 mM, 2 mM, and 4 mM D-GlcNAc in MCF-7 and 4T1 cell lines compared with untreated cell cultures (*P <0.01-P <0.0001*) (**Figure 2**). Cancerogenic cell survival significantly decreased with 0.5 mM, 1 mM, 2 mM, and 4 mM D-GlcNAc in 4T1, and 1 mM, 2 mM, and 4 mM D-GlcNAc in MCF-7 cells compared with untreated cell cultures (*P <0.01-P <0.0001*). The early apoptotic cells were significantly increased with 0.5 mM, 1 mM, 2 mM, and 4 mM D-GlcNAc in 4T1, and 1 mM, 2 mM, and 4 mM D-GlcNAc in MCF-7 cells compared with untreated cell cultures (*P <0.01-P <0.0001*). The late apoptotic cells did not significantly change in MCF-7 cells cultured with D-GlcNAc (*P <0.01-P <0.0001*) but significantly decreased with 1 mM, 2 mM, and 4 mM D-GlcNAc in 4T1 cells compared to untreated cell cultures (*P <0.01-P <0.0001*). The total apoptotic cells significantly increased with 0.5 mM, 1 mM, 2 mM, and 4 mM D-GlcNAc in 4T1 cells and 1 mM, 2 mM, and 4 mM D-GlcNAc in MCF-7 cells compared with untreated cell cultures (*P <0.01-P <0.0001*) (**Figure 3, Figure 4**).

3.3. D-GlcNAc reduced tumor size and angiogenesis in the breast cancer murine model

Histopathological analysis showed a significant reduction in the tumor size, mitosis, and angiogenesis in the D-GlcNAc post-treatment group compared with the breast cancer group (P <0.01-P <0.0001). Also, mitosis has decreased compared to the control group, but the cause of standard deviation was not significantly different. Inflammation was also increased in the D-GlcNAc pre-treatment group compared with the breast cancer group (P <0.01). Necrosis and Pleomorphism tended to decrease in the D-GlcNAc post-treatment group compared with the breast cancer group, but no significant difference was observed among the groups (**Figure 5**).

3.4. Molecular docking and dynamic analysis

Molecular docking of D-GlcNAc to HER2 resulted in affinity scores of -6.2 and -6.4 as repetitive experiments, respectively. A close inspection of the interaction interface also reveals critical interactions, including hydrogen bond pairs that could be responsible for this high affinity (details of the interactions and distances, residues and atoms involved are included in Supplementary Materials S6). The HER2 Cα RMSD in the simulation system remained stable with RMSD < 3 Å throughout the simulation period. HER2 Cα RMSD gradually increased as the simulation regressed (**Figure 6**A). This gradual increase in the RMSD showed the presence of many loop motifs in the HER2 structure (this phenomenon is visible in Supplementary Materials S7). D-GlcNAc, on the other hand, completely deviated from its docked pose with HER2 (RMSD > 20 Å) and failed to validate the docked pose. However, D-GlcNAc simulated with HER2 showed relatively stable RMSD as the simulation progressed (**Figure 6**B). The affinity of D-GlcNAc with HER2 can further be correlated to the hydrogen bonds it formed. Likewise, the lack of affinity of D-GlcNAc with HER2 could be validated by the reduction of hydrogen bond pairs as the simulation regressed (**Figure 6**C). The results in Figure **7** show D-GlcNAc as a potential inhibitor of HER2, whereas it provides computational results to validate the role of D-GlcNAc as a potential antagonist for the HER2 that further could be the underlying basis for the former anti-tumoral activity.

4. Discussion

N-acetylglucosamine is an essential amino sugar moiety for protein glycosylation [41]. Glycosylation, a posttranslational protein modification, plays a crucial biological role in many physiological and pathological events [42]. In studies, N-glycan changes have been detected during breast cancer progression [43]. In particular, numerous studies have focused on the dysregulated glycosylation involved in the development and progression of breast cancer [44, 45]. Previous studies concluded that control of glycosylation could be a practical treatment approach for cancer progression [46]. Therefore, regulation of glycosylation is an essential process for breast cancer and many types of cancer [46, 47].

Glucosamine plays an essential role in cancer treatment. Daily glucosamine injection has reduced cell mass and large haemorrhagic areas in Sarcoma 37 tumors in mice [48]. Although glucosamine treatment did not result in complete tumor regression, approximately double the survival time of treated mice has been reported [49]. Additionally, in a study investigating the protective effect of glucosamine, a linkage

was observed between the use of glucosamine and a lower risk of lung and colorectal cancer [50]). It is known that O-linked N-acetylglucosaminylation (O-GlcNAcylation) is a reversible posttranslational modification of serine/threonine residues and that the O-linked N-acetyl-glucosamine transferase enzyme mediates O-GlcNAsylation of various proteins involved in cervical cancer tumorigenesis [51]. Alteration of protein glycosylation has been correlated with tumorigenesis, but the effect of regulation of glycosylation on tumor development remains unclear [8].

Our study focused on the immune system modulator effect of D-GlcNAc as a candidate supplement compound against breast cancer. An administrative dose was determined using the machine learning method (Table 1), which was later applied *in vitro* to MCF-7 and 4T1 cell lines, as the most common breast cancer cell lines with *in vivo* to xenograft murine model. *In vitro*, results demonstrated that D-GlcNAc inhibits cell proliferation by promoting apoptosis in MCF-7 and 4T1 cell lines in a concentration-dependent manner and following our findings, in another study, overexpressed MGAT3 in breast cancer MDA-MB-231 cells which leads to bisecting of N-GlcNAc, which causes suppression on the EGFR/Erk signalling and reduced migratory ability, cell proliferation, and clonal formation [45].

Our *in vitro* results showed promoted apoptosis and Fas expression in MCF-7 and 4T1 cell lines depending on the increasing concentrations of D-GlcNAc, and accordingly suppressed proliferation in cancer cells. Furthermore, the data have been consistent with the hypothesis of our studies using the machine learning method, which has indicated 2 mM D-GlcNAc as the cut-off level for apoptosis, Fas expression, and proliferation rate were confirmed with *in vitro* results. Therefore, we have used 2 mM D-GlcNAc to treat the xenograft murine model.

In a previous study, abnormal glycosylation correlated with N-glycan alterations in breast cancer cells compared to normal cells [52]. In addition, GlcNAc and glucosamine (GlcN) have been used as contrast agents to detect breast tumors, by targeting tumor cells using magnetic resonance imaging [53]. Afterwards, a study closely related to our findings indicated that GlcNAc sensitizes non-small cell lung cancer cells (NSCLC) via TRAIL-induced apoptosis, which can be a novel effective agent for TRAIL-mediated NSCLC-targeted therapy [4]. Since the tumor growth and metastatic spread of 4T1 cells in BALB/c mice closely mimic human breast cancer, we have preferred applying the 4T1 mouse model. The D-GlcNAc was administered on the 1st day or 18th day after inoculation of 4T1 cells to evaluate the pre-tumoral and post-tumoral effect of D-GlcNAc. The *in vivo* results demonstrated that D-GlcNAc could reduce tumor size, mitosis, and angiogenesis in the post-treatment group, which could indicate the tumour-targeted effect of D-GlcNAc.

Sialylations mediate signaling, immunological responses, and cell-cell interactions in normal cells. However, abnormalities in sialylations can occur due to mutated genes, altered gene expressions, or defective enzymes involved in metabolism, including sialyltransferases and sialidases. They affect sialic acid metabolism and normal sialylation of glycoproteins and glycolipids associated with diseases. Sialic acid is a biomarker of several diseases, including cancer [54]. Sialylation generally increases in tumor cells and is incorporated with N-glycans and O-glycans. N-glycan sialylation could serve as a regulatory

mechanism for various receptor tyrosine kinases, as shown by following the activation of MET and RON receptors by α2-3Sia.

Contrary to the effect of galectins, death receptor ligands, and chemotherapeutic drugs inducing apoptosis, increase α2-6Sia on N-glycans because ST6GAL1 up-regulation in cancer cells enhances integrin-mediated cell motility and protects cells against apoptosis [7]. Here, we have assumed a reversible effect of exogenously administered D-GlcNAc that removes cells' protection against apoptosis by binding on HER2 protein (Fig. 6, Fig. 7**)**. Furthermore, in a previous study, HER2 showed an inhibitory role in the cGAS–STING-Mediated immune response, which causes DNA damage [55]. Our presented data with molecular docking and dynamics analysis have proved that the binding of D-GlcNAc to HER2 could be associated with preventing DNA damage (Fig. 6, Fig. 7). *In vitro* assays and murine model studies have supported our hypothesis according to the induced apoptosis in D-GlcNAc-administered cancer cell lines (Fig. 4, Fig. 5**)**.

The predicted interferences related to the induction of tumor progression involving β1–4 branched tetra-antennary N-glycan formation by MGAT4 expression enhances lattice formation via galectin binding to poly-N-acetyllactosamines [7]. The exogenously D-GlcNAc administration could result in the displacement of Galactin, and D-GlcNAc's binding on HER2 could revert tumor progression into the recession phase due to apoptosis and cell death.

The cancer cells spread throughout the body and show high metastasizing, which can avoid detection and neutralization by the immune system. This case relies on mimicking the glycosylation patterns of healthy immune cells, which is the reason for self-signalling and avoiding the immune system attack. Sialylation converts the surface of cancer cells to prime ligands for sialic acid-binding immunoglobulin-type lectins (Siglecs), similar to the immune cells' surface architecture [56, 57]. Bounding to sialylated glycans produces Siglecs promotion due to immunosuppressive signalling and protects the tumour cell [58–60]. Therefore, natural killer (NK)-cell-mediated tumor cell death was inhibited by interactions between NK-expressed Siglec-7 or Siglec-9 and sialylated glycans (Siglec ligands), which leads to the hiding of tumor cells from immune cells [61, 62]. In previous studies, monoclonal antibodies targeting Siglec-7 and Siglec-9 have been suggested to neutralize Siglec–Siglec ligand interactions [63]. This study showed that the binding of Siglec-9-expressing macrophages plays a role in the induction of a tumour-associated macrophage phenotype that has primed the myeloid cells to release factors that promote disease progression (such as interleukin 6 and macrophage colony-stimulating factor) that are based on soluble mucin-1 and mucin-1 expressed on T47D breast cancer cells [63, 64]. Multiple myeloma cells are possible, which bind to Siglec-7 and Siglec-9 and avoid NK cells. Still, once the sialic acid residues treat with neuraminidase or inhibited by sialylation using the sialyltransferase inhibitor 3Fax-Neu5Ac34, NK cells can kill multiple myeloma cells [65].

The cancer cells hide from immune defence cells by mimicking the sialic acid-binding immunoglobulin(Ig)-like lectins, which are the members of the immunoglobulin superfamily, and act like immune regulatory receptors on the transmembrane cell surface. Consequently, sialic acid-binding sites

activate or inhibit the immune response [66]. In the insights of previous findings related to sialic acid-binding Ig-like lectin mechanisms, our study showed that D-GlcNAc could compensate for lectin, previously desired in the sialic acid-binding Ig lectin mechanism. We suggested that the cancer cells could be deceived and directed to apoptosis by the presence of D-GlcNAc. As parameters related to the inhibition of cancerogenic cells, we have observed a significant decrease in metastasis and an increase in apoptosis and Fas expression on D-GlcNAc treated cells (Fig. 1, Fig. 2, Fig. 3, Fig. 4, Fig. 5). We have also observed a veinal decrease and recession of metastasis in mice murine model studies, which could be associated with the positive effect of D-GlcNAc.

Alternatively, factor H limiting activation and modulation of tumour cells helps for metastasis and suppresses antitumour immunity by inhibition of Siglecs. Some tumour cells express de-N-acetyl (deNAc) gangliosides, which protect tumour cells from apoptosis and activate the epidermal growth factor receptor (EGFR). Mucins could prevent intercellular interactions and inhibit cadherins and integrins from functioning, resulting in apoptosis. Hence, they might block and mask recognition by major histocompatibility complex molecules [7]. Mucin secretion results from the loss of normal topology and polarisation of epithelial cells in cancer due to impairment of O-GalNAc molecule structure. Tumour cells attack tissues and the bloodstream when they have mucin on their cell surfaces. O-GlcNAc levels are altered in many cancers, which serve as a nutrient sensor to regulate signalling, transcription, mitochondrial activity, and cytoskeletal functions [67, 68]. Since this case activates EGF or IGF-1 signalling, we assumed it to have a reversible effect of D-GlcNAc, leading breast cancer to apoptosis and Fas expression (Fig. 2, Fig. 3).

O-GlcNAcylation influences cancer cell metabolism due to changes in the stability or activity of transcription factors and kinases, which the administration of D-GlcNAc could modulate. In recent studies, the findings on targeting glycan-dependent molecular interactions have attracted researchers' attention to enhance the immune system. The sialoglycan–Siglec interaction displays another critical point of view of the immune checkpoint. A function-blocker and modulator compound introduced to replace Siglecs, such as lectin precursor GlcNAc, could be suggested [69, 70]. Therefore, D-GlcNAc could be considered and tested in clinical studies on account of its potential effect by combining with other approved methods and anticancer drugs developed to block tumour cells via administration of sialic acid mimetics or the targeted delivery of sialidases to tumour cell surfaces [69].

Our findings reveal a major role of D-GlcNAc, which is necessary for activating the immune system resulting in early apoptosis and recession in metastasis that we have observed in our mice murine model. O-GlcNAc transferase enzyme (OGT) functions on UDP-GlcNAc as a nuclear and cytoplasmic metabolism substrate. This interaction increases in multiple cancers, and a decrease in OGT level blocks tumour growth. Previous studies have reported MannaC as an inhibitor of sialic acid in cancer cells. We have predicted the impairment in the mechanism related to converting UDP-GlcNAc to Mannac. Therefore, it does not work as a sialic acid inhibitor, preventing apoptosis and Fas expression. However, D-GlcNAc could not be utilized by cancer cells and decrease the transferase enzyme, which could reduce metastasis and veining as we have observed in mice murine model studies [70–72]. As reported in a previous study,

the viral agents' energy consumption, the predicted reason for breast cancer, and HCMV infection did not increase intracellular UDP-sugar metabolite pools. However, this process induced UDP-sugar biosynthesis depending on UDP-glucose and the biosynthetic flux of UDP-GlcNAc. This study suggested the role of sugar metabolism, which induced peculiar to HCMV infection [73]. Consistent with this finding, Pan et al. [74] showed upregulation of UDP-glucose dehydrogenase gene expression via ERK and PI3K/Akt pathway due to EBV latent membrane protein 2A detected in nasopharyngeal carcinoma. These findings demonstrate a linkage between virus infection and cancer formation depending on glycosylation pathways in the cell. As published in our previous studies, the stimulative effect of D-GlcNAc can potentially increase the defence capacity of the immunological response to SARS-CoV-2 [9, 10]. Moreover, N-acetyl-D-glucosamine-coated poly(amidoamine) structures have also induced upregulation of antibody formation in the rat recombinant cells [75], which could be a predicted response as expected in the human cell.

In accordance with our study, Denning et al. [76] showed that ROS induces Fas expression, which causes apoptosis in intestinal epithelial cells. In D-GlcNAc treated cells, we have observed higher Fas expression than untreated cells. ROS-induced Fas expression could be the reason for oxidative stress exposure to breast cancer due to D-GlcNAc administration. Moreover, oxidative stress causes starvation on cell growth, which activates Fas expression leading to apoptosis [77]. In our study, the higher Fas expression in D-GlcNAc treated cells and the increased apoptotic rate could be suggested triggering of apoptotic pathways and enhancing Necrosis on cancer cells depending on D-GlcNAc administration (Fig. 2, Fig. 3, Fig. 4, Fig. 5).

5. Conclusion

Our findings demonstrate the potential of D-GlcNAc as a treatment approach to decrease mammary gland tumour cell proliferation, characterized by increased Fas expression and induction of early apoptosis. Moreover, we observed that exogenous administration of D-GlcNAc can reduce mitosis and angiogenesis in breast cancer cells. Notably, the reduction in tumor size observed in our murine model warrants further investigation to assess the potential synergistic effects of D-GlcNAc in combination with conventional therapies for breast cancer treatment.

Considering the lack of cytostatic effects reported in FDA documentation, future studies should explore the synergistic effects of D-GlcNAc in combination with approved anticancer drugs, considering appropriate and reasonable doses within the concentration range we tested (mM level). Given its promising therapeutic properties, these preclinical findings support the need for further clinical studies involving D-GlcNAc administration. Clinical trials are necessary to determine the efficacy and safety profile of D-GlcNAc as an adjunct therapy in breast cancer treatment.

Declarations

AUTHOR CONTRIBUTIONS

Ömür Baysal: Conceptualisation (lead); Data curation (lead); Formal analysis (lead); Methodology (equal); Supervision (lead); Writing – original draft (lead); Writing – review & editing (lead).**Deniz Genç:** Formal analysis (lead); Methodology (lead).**Ragıp Soner Silme:** Conceptualisation (equal); Methodology (supporting); Writing – original draft (lead); Writing – review & editing (lead).**Kevser Kübra Kırboga**: Conceptualisation (equal); Methodology (supporting). **Dilek** Ç**oban:** Formal analysis (equal),Methodology (supporting); **Naeem Abdul Ghafoor:** Formal analysis (equal); Methodology (supporting).**Leyla Tekin:** Formal analysis (lead); Methodology (equal).**Osman Bulut:** Formal analysis (equal); Methodology (supporting).

ACKNOWLEDGMENT

This study is dedicated to the memory of late Ali Rıza Baysal (grandfather of Dr Baysal) who was diagnosed with throat cancer and lost his vocal cords, and to all other patients battling with various cancer types. The patenting procedures supported by Muğla Sıtkı Koçman University, Scientific Research Projects (BAP) on this presented compound and its immunomodulatory effect was initiated by the Turkish Patent and Trademark Office (Pat.No: TR Patent 2022-GE-992366/ 2022/021652).

DATA AVAILABILITY STATEMENT

Data associated with this study are summarised in the manuscript or included in the Supplemental information.

FUNDING STATEMENT

This research did not receive any specific grant from funding agencies in the public, commercial, or not-for-profit sectors.

CONFLICT OF INTEREST

The authors declare that they have no known competing financial interests or personal relationships that could have appeared to influence the work reported in this paper.

ETHICS STATEMENT

The current research was approved by the the Muğla Sıtkı Koçman University Experimental Animal Center.

PATIENT CONSENT STATEMENT

Not required.

References

1. Lovrics O et al (Oct 2021) The effect of bariatric surgery on breast cancer incidence and characteristics: A meta-analysis and systematic review," (in eng). Am J Surg 222(4):715–722.

10.1016/j.amjsurg.2021.03.016

2. Maughan KL, Lutterbie MA, Ham PS (Jun 1 2010) Treatment of breast cancer," (in eng). Am Fam Physician 81(11):1339–1346
3. Bhushan A, Gonsalves A, Menon JU (2021) "Current State of Breast Cancer Diagnosis, Treatment, and Theranostics," (in eng), *Pharmaceutics*, vol. 13, no. 5, May 14 doi: 10.3390/pharmaceutics13050723
4. Liang Y et al (2018) N-Acetyl-Glucosamine Sensitizes Non-Small Cell Lung Cancer Cells to TRAIL-Induced Apoptosis by Activating Death Receptor 5," (in eng). Cell Physiol Biochem 45(5):2054–2070. 10.1159/000488042
5. Mattaveewong T, Wongkrasant P, Chanchai S, Pichyangkura R, Chatsudthipong V, Muanprasat C (2016) "Chitosan oligosaccharide suppresses tumor progression in a mouse model of colitis-associated colorectal cancer through AMPK activation and suppression of NF-κB and mTOR signaling," (in eng), *Carbohydr Polym*, vol. 145, pp. 30 – 6, Jul 10 doi: 10.1016/j.carbpol.2016.02.077
6. Medina SH, Tekumalla V, Chevliakov MV, Shewach DS, Ensminger WD, El-Sayed ME (2011) "N-acetylgalactosamine-functionalized dendrimers as hepatic cancer cell-targeted carriers," (in eng), *Biomaterials*, vol. 32, no. 17, pp. 4118-29, Jun doi: 10.1016/j.biomaterials.2010.11.068
7. Varki A, Kannagi R, Toole B, Stanley P et al (2015) "Glycosylation Changes in Cancer," in *Essentials of Glycobiology*, A. Varki Eds. Cold Spring Harbor (NY): Cold Spring Harbor Laboratory Press Copyright 2015–2017 by The Consortium of Glycobiology Editors, La Jolla, California. All rights reserved., pp. 597–609
8. Chou TY, Hart GW (2001) "O-linked N-acetylglucosamine and cancer: messages from the glycosylation of c-Myc," (in eng), *Adv Exp Med Biol*, vol. 491, pp. 413-8, doi: 10.1007/978-1-4615-1267-7_26
9. Baysal Ö, Silme R, Karaaslan C (2020) *Genetic Uniformity of a Specific Region in SARS-CoV-2 Genome and In-Silico Target-Oriented Repurposing of N-Acetyl-D-Glucosamine*.
10. Baysal Ö, Abdul Ghafoor N, Silme RS, Ignatov AN, Kniazeva V (2021) Molecular dynamics analysis of N-acetyl-D-glucosamine against specific SARS-CoV-2's pathogenicity factors. PLoS ONE 16(5):e0252571. 10.1371/journal.pone.0252571
11. Buehring GC, Shen HM, Jensen HM, Choi KY, Sun D, Nuovo G (May 2014) Bovine leukemia virus DNA in human breast tissue," (in eng). Emerg Infect Dis 20(5):772–782. 10.3201/eid2005.131298
12. Buehring GC, Shen HM, Jensen HM, Jin DL, Hudes M, Block G (2015) Exposure to Bovine Leukemia Virus Is Associated with Breast Cancer: A Case-Control Study," (in eng). PLoS ONE 10(9):e0134304. 10.1371/journal.pone.0134304
13. Melana SM et al (2010) "Detection of human mammary tumor virus proteins in human breast cancer cells," (in eng), *J Virol Methods*, vol. 163, no. 1, pp. 157 – 61, Jan doi: 10.1016/j.jviromet.2009.09.015
14. Tsai JH et al (Jan 2007) Relationship between viral factors, axillary lymph node status and survival in breast cancer," (in eng). J Cancer Res Clin Oncol 133(1):13–21. 10.1007/s00432-006-0141-5

15. Joshi D, Quadri M, Gangane N, Joshi R, Gangane N (2009) Association of Epstein Barr Virus Infection (EBV) with Breast Cancer in Rural Indian Women. PLoS ONE 4(12):e8180. 10.1371/journal.pone.0008180
16. Fawzy S, Sallam M, Awad NM "Detection of Epstein-Barr virus in breast carcinoma in Egyptian women," (in eng), Clin Biochem, vol. 41, no. 7–8, pp. 486 – 92, May 2008, doi: 10.1016/j.clinbiochem.2007.12.017
17. Hachana M, Amara K, Ziadi S, Romdhane E, Gacem RB, Trimeche M "Investigation of Epstein-Barr virus in breast carcinomas in Tunisia," (in eng), *Pathol Res Pract*, vol. 207, no. 11, pp. 695–700, Nov 15 2011, doi: 10.1016/j.prp.2011.09.007
18. Harkins LE et al (2010) "Detection of human cytomegalovirus in normal and neoplastic breast epithelium," (in eng), *Herpesviridae*, vol. 1, no. 1, p. 8, Dec 23 doi: 10.1186/2042-4280-1-8
19. Taher C et al (2013) "High prevalence of human cytomegalovirus proteins and nucleic acids in primary breast cancer and metastatic sentinel lymph nodes," (in eng), *PLoS One*, vol. 8, no. 2, p. e56795, doi: 10.1371/journal.pone.0056795
20. Costa H et al "Human cytomegalovirus infection is correlated with enhanced cyclooxygenase-2 and 5-lipoxygenase protein expression in breast cancer," (in eng), J Cancer Res Clin Oncol, vol. 145, no. 8, pp. 2083–2095, Aug 2019, doi: 10.1007/s00432-019-02946-8
21. Yang Z et al (2019) "Latent Cytomegalovirus Infection in Female Mice Increases Breast Cancer Metastasis," (in eng), *Cancers (Basel)*, vol. 11, no. 4, Mar 29 doi: 10.3390/cancers11040447
22. Alibek K, Kakpenova A, Mussabekova A, Sypabekova M, Karatayeva N (2013) Role of viruses in the development of breast cancer," (in eng). Infect Agent Cancer 8:32. 10.1186/1750-9378-8-32
23. Richardson A (1997) "Is breast cancer caused by late exposure to a common virus?," (in eng), *Med Hypotheses*, vol. 48, no. 6, pp. 491-7, Jun doi: 10.1016/s0306-9877(97)90118-3
24. Carpenter RL, Lo HW (2013) "Regulation of Apoptosis by HER2 in Breast Cancer," (in eng), *J Carcinog Mutagen*, vol. no. Suppl 7, 2013, doi: 10.4172/2157-2518.S7-003
25. Gaulton A et al (2017) "The ChEMBL database in 2017," (in eng), *Nucleic Acids Res*, vol. 45, no. D1, pp. D945-d954, Jan 4 doi: 10.1093/nar/gkw1074
26. Jaeger S, Fulle S, Turk S "Mol2vec: Unsupervised Machine Learning Approach with Chemical Intuition," J Chem Inf Model, vol. 58, no. 1, pp. 27–35, 2018/01/22 2018, doi: 10.1021/acs.jcim.7b00616
27. Huang K, Fu T, Glass LM, Zitnik M, Xiao C, Sun J (2021) "DeepPurpose: a deep learning library for drug-target interaction prediction," (in eng), *Bioinformatics*, vol. 36, no. 22–23, pp. 5545–5547, Apr 1 doi: 10.1093/bioinformatics/btaa1005
28. *RDKit: Open-source cheminformatics*. [Online]. Available: https://www.rdkit.org/
29. Pedregosa F et al "Scikit-learn: Machine Learning in Python," *arXiv pre-print server*, 2018-06-05 2018, doi: None arxiv:1201.0490

30. Cucina A et al (2009) "Evidence for a biphasic apoptotic pathway induced by melatonin in MCF-7 breast cancer cells," (in eng), *J Pineal Res*, vol. 46, no. 2, pp. 172 – 80, Mar doi: 10.1111/j.1600-079X.2008.00645.x
31. Matera G, Lupi M, Ubezio P (2004) "Heterogeneous cell response to topotecan in a CFSE-based proliferation test," (in eng), *Cytometry A*, vol. 62, no. 2, pp. 118 – 28, Dec doi: 10.1002/cyto.a.20097
32. Pulaski BA, Ostrand-Rosenberg S "Mouse 4T1 Breast Tumor Model," *Current Protocols in Immunology*, https://doi.org/10.1002/0471142735.im2002s39 vol. 39, no. 1, pp. 20.2.1–20.2.16, 2000/10/01 2000, doi: https://doi.org/10.1002/0471142735.im2002s39
33. Zheng L et al (Dec 2014) A model of spontaneous mouse mammary tumor for human estrogen receptor- and progesterone receptor-negative breast cancer," (in eng). Int J Oncol 45(6):2241–2249. 10.3892/ijo.2014.2657
34. Morris GM et al (Dec 2009) AutoDock4 and AutoDockTools4: Automated docking with selective receptor flexibility," (in eng). J Comput Chem 30(16):2785–2791. 10.1002/jcc.21256
35. Trott O, Olson AJ (2010) "AutoDock Vina: improving the speed and accuracy of docking with a new scoring function, efficient optimization, and multithreading," (in eng), *J Comput Chem*, vol. 31, no. 2, pp. 455 – 61, Jan 30 doi: 10.1002/jcc.21334
36. Grosdidier A, Zoete V, Michielin O (Jul 2011) SwissDock, a protein-small molecule docking web service based on EADock DSS," (in eng). Nucleic Acids Res 39 Web Server issue, pp. W270-7. 10.1093/nar/gkr366
37. Phillips JC et al (Jul 28 2020) Scalable molecular dynamics on CPU and GPU architectures with NAMD," (in eng). J Chem Phys 153(4):044130. 10.1063/5.0014475
38. Huang J et al (Jan 2017) CHARMM36m: an improved force field for folded and intrinsically disordered proteins," (in eng). Nat Methods 14(1):71–73. 10.1038/nmeth.4067
39. Lee J et al (2016) "CHARMM-GUI Input Generator for NAMD, GROMACS, AMBER, OpenMM, and CHARMM/OpenMM Simulations Using the CHARMM36 Additive Force Field," (in eng), *J Chem Theory Comput*, vol. 12, no. 1, pp. 405 – 13, Jan 12 doi: 10.1021/acs.jctc.5b00935
40. Gowers R et al (2016) "MDAnalysis: A Python Package for the Rapid Analysis of Molecular Dynamics Simulations," : SciPy, doi: 10.25080/majora-629e541a-00e. [Online]. Available: https://dx.doi.org/10.25080/majora-629e541a-00e
41. Ma J, Hart GW "O-GlcNAc profiling: from proteins to proteomes," *Clinical Proteomics*, vol. 11, no. 1, p. 8, 2014/03/05 2014, doi: 10.1186/1559-0275-11-8
42. Elola M et al (2016) "Glycosylation-dependent binding of galectin-8 to activated leukocyte cell adhesion molecule (ALCAM/CD166) promotes its surface segregation on breast cancer cells. Fernández MM, Ferragut F, Cárdenas Delgado VM, Bracalente C, Bravo AI, Cagnoni AJ, Nuñez M, Morosi LG, Quinta HR, Espelt MV, Troncoso MF, Wolfenstein-Todel C, Mariño KV, Malchiodi EL, Rabinovich GA, Elola MT. Biochim Biophys Acta. Apr 26. pii: S0304-4165(16)30124-6. doi: 10.1016/j.bbagen.2016.04.019. [Epub ahead of print]," *Biochimica et Biophysica Acta (BBA) - General Subjects*, 04/26 2016

43. Peixoto A, Relvas-Santos M, Azevedo R, Santos LL, Ferreira JA (2019) Protein Glycosylation and Tumor Microenvironment Alterations Driving Cancer Hallmarks," (in English). Front Oncol Rev vol 9. 2019-May-1410.3389/fonc.2019.00380
44. Kumar P, Tambe P, Paknikar KM, Gajbhiye V (Aug 1 2017) Folate/N-acetyl glucosamine conjugated mesoporous silica nanoparticles for targeting breast cancer cells: A comparative study," (in eng). Colloids Surf B Biointerfaces 156:203–212. 10.1016/j.colsurfb.2017.05.032
45. Cheng L et al "Bisecting N-Acetylglucosamine on EGFR Inhibits Malignant Phenotype of Breast Cancer via Down-Regulation of EGFR/Erk Signaling," (in English), *Frontiers in Oncology*, Original Research vol. 10, 2020-June-16 2020, doi: 10.3389/fonc.2020.00929
46. Mereiter S, Balmaña M, Campos D, Gomes J, Reis CA "Glycosylation in the Era of Cancer-Targeted Therapy: Where Are We Heading?," (in eng), *Cancer Cell*, vol. 36, no. 1, pp. 6–16, Jul 8 2019, doi: 10.1016/j.ccell.2019.06.006
47. Xu W, Jiang C, Kong X, Liang Y, Rong M, Liu W "Chitooligosaccharides and N-acetyl-D-glucosamine stimulate peripheral blood mononuclear cell-mediated antitumor immune responses," Mol Med Rep, vol. 6, no. 2, pp. 385–390, 2012/08/01 2012, doi: 10.3892/mmr.2012.918
48. Quastel JH, Cantero A "Inhibition of Tumour Growth by D-Glucosamine," Nature, vol. 171, no. 4345, pp. 252–254, 1953/02/01 1953, doi: 10.1038/171252a0
49. Brasky TM, Lampe JW, Slatore CG, White E (Sep 2011) Use of glucosamine and chondroitin and lung cancer risk in the VITamins And Lifestyle (VITAL) cohort," (in eng). Cancer Causes Control 22(9):1333–1342. 10.1007/s10552-011-9806-8
50. Kantor ED, Lampe JW, Peters U, Shen DD, Vaughan TL, White E (Jun 2013) Use of glucosamine and chondroitin supplements and risk of colorectal cancer," (in eng). Cancer Causes Control 24(6):1137–1146. 10.1007/s10552-013-0192-2
51. Kim MJ et al (2018) "O-linked N-acetylglucosamine transferase enhances secretory clusterin expression via liver X receptors and sterol response element binding protein regulation in cervical cancer," (in eng), *Oncotarget*, vol. 9, no. 4, pp. 4625–4636, Jan 12 doi: 10.18632/oncotarget.23588
52. Taniguchi N, Kizuka Y (2015) Glycans and cancer: role of N-glycans in cancer biomarker, progression and metastasis, and therapeutics," (in eng). Adv Cancer Res 126:11–51. 10.1016/bs.acr.2014.11.001
53. Rivlin M, Navon G (Sep 7 2016) Glucosamine and N-acetyl glucosamine as new CEST MRI agents for molecular imaging of tumors. (in eng) Sci Rep 6:32648. 10.1038/srep32648
54. Ghosh S (2020) Chapter 9 - Sialic acids and sialoglycans in endocrinal disorders. Sialic Acids and Sialoglycoconjugates in the Biology of Life, Health and Disease. S. Ghosh Ed.: Academic Press, pp 247–268
55. Wu S et al (2019) "HER2 recruits AKT1 to disrupt STING signalling and suppress antiviral defence and antitumour immunity," (in eng), *Nat Cell Biol*, vol. 21, no. 8, pp. 1027–1040, Aug doi: 10.1038/s41556-019-0352-z
56. Läubli H, Varki A (Feb 2020) Sialic acid-binding immunoglobulin-like lectins (Siglecs) detect self-associated molecular patterns to regulate immune responses," (in eng). Cell Mol Life Sci 77(4):593–

605. 10.1007/s00018-019-03288-x

57. Crocker PR, Paulson JC, Varki A (2007) Siglecs and their roles in the immune system. Nat Rev Immunol 7(4):255–266 2007/04/01. 10.1038/nri2056
58. Macauley MS, Crocker PR, Paulson JC (2014) Siglec-mediated regulation of immune cell function in disease. Nat Rev Immunol 14(10):653–666. 10.1038/nri3737. /10/01 2014
59. Rambaruth ND, Dwek MV (2011) "Cell surface glycan-lectin interactions in tumor metastasis," (in eng), *Acta Histochem*, vol. 113, no. 6, pp. 591–600, Oct doi: 10.1016/j.acthis.2011.03.001
60. van de Wall S, Santegoets KCM, van Houtum EJH, Büll C, Adema GJ (2020) "Sialoglycans and Siglecs Can Shape the Tumor Immune Microenvironment," (in eng), *Trends Immunol*, vol. 41, no. 4, pp. 274–285, Apr doi: 10.1016/j.it.2020.02.001
61. Hudak JE, Canham SM, Bertozzi CR (Jan 2014) Glycocalyx engineering reveals a Siglec-based mechanism for NK cell immunoevasion," (in eng). Nat Chem Biol 10(1):69–75. 10.1038/nchembio.1388
62. Daly J, Carlsten M, O'Dwyer M (2019) Sugar Free: Novel Immunotherapeutic Approaches Targeting Siglecs and Sialic Acids to Enhance Natural Killer Cell Cytotoxicity Against Cancer," (in eng). Front Immunol 10:1047. 10.3389/fimmu.2019.01047
63. Bärenwaldt A, Läubli H (Oct 2019) The sialoglycan-Siglec glyco-immune checkpoint - a target for improving innate and adaptive anti-cancer immunity," (in eng). Expert Opin Ther Targets 23(10):839–853. 10.1080/14728222.2019.1667977
64. Beatson R et al (Nov 2016) The mucin MUC1 modulates the tumor immunological microenvironment through engagement of the lectin Siglec-9," (in eng). Nat Immunol 17(11):1273–1281. 10.1038/ni.3552
65. Rillahan CD et al (Jul 2012) Global metabolic inhibitors of sialyl- and fucosyltransferases remodel the glycome," (in eng). Nat Chem Biol 8(7):661–668. 10.1038/nchembio.999
66. Horstkorte R, Fuss B (2012) Chapter 9 - Cell Adhesion Molecules. In: Brady ST, Siegel GJ, Albers RW, Price DL (eds) Basic Neurochemistry (Eighth Edition). Academic Press, New York, pp 165–179
67. Hart GW "Nutrient regulation of signaling and transcription," (in eng), J Biol Chem, vol. 294, no. 7, pp. 2211–2231, Feb 15 2019, doi: 10.1074/jbc.AW119.003226
68. Chugh S, Gnanapragassam VS, Jain M, Rachagani S, Ponnusamy MP, Batra SK (2015) "Pathobiological implications of mucin glycans in cancer: Sweet poison and novel targets," (in eng), *Biochim Biophys Acta*, vol. 1856, no. 2, pp. 211 – 25, Dec doi: 10.1016/j.bbcan.2015.08.003
69. Pietrobono S, Stecca B (2021) "Aberrant Sialylation in Cancer: Biomarker and Potential Target for Therapeutic Intervention?," (in eng), *Cancers (Basel)*, vol. 13, no. 9, Apr 22 doi: 10.3390/cancers13092014
70. Akella NM et al (Apr 2020) O-GlcNAc Transferase Regulates Cancer Stem-like Potential of Breast Cancer Cells," (in eng). Mol Cancer Res 18(4):585–598. 10.1158/1541-7786.Mcr-19-0732

71. Ma Z, Vosseller K (2014) "Cancer metabolism and elevated O-GlcNAc in oncogenic signaling," (in eng), *J Biol Chem*, vol. 289, no. 50, pp. 34457-65, Dec 12 doi: 10.1074/jbc.R114.577718
72. Lam C, Low JY, Tran PT, Wang H "The hexosamine biosynthetic pathway and cancer: Current knowledge and future therapeutic strategies," (in eng), Cancer Lett, vol. 503, pp. 11–18, Apr 10 2021, doi: 10.1016/j.canlet.2021.01.010
73. DeVito SR, Ortiz-Riaño E, Martínez-Sobrido L, Munger J (2014) "Cytomegalovirus-mediated activation of pyrimidine biosynthesis drives UDP-sugar synthesis to support viral protein glycosylation," (in eng), *Proc Natl Acad Sci U S A*, vol. 111, no. 50, pp. 18019-24, Dec 16 doi: 10.1073/pnas.1415864111
74. Pan YR, Vatsyayan J, Chang YS, Chang HY (Dec 2008) Epstein-Barr virus latent membrane protein 2A upregulates UDP-glucose dehydrogenase gene expression via ERK and PI3K/Akt pathway," (in eng). Cell Microbiol 10(12):2447–2460. 10.1111/j.1462-5822.2008.01221.x
75. Hulikova K, Benson V, Svoboda J, Sima P, Fiserova A (2009) "N-Acetyl-D-glucosamine-coated polyamidoamine dendrimer modulates antibody formation via natural killer cell activation," (in eng), *Int Immunopharmacol*, vol. 9, no. 6, pp. 792-9, Jun doi: 10.1016/j.intimp.2009.03.007
76. Denning TL, Takaishi H, Crowe SE, Boldogh I, Jevnikar A, Ernst PB (2002) "Oxidative stress induces the expression of Fas and Fas ligand and apoptosis in murine intestinal epithelial cells," (in eng), *Free Radic Biol Med*, vol. 33, no. 12, pp. 1641-50, Dec 15 doi: 10.1016/s0891-5849(02)01141-3
77. Brunk UT, Svensson I (1999) Oxidative stress, growth factor starvation and Fas activation may all cause apoptosis through lysosomal leak," (in eng). Redox Rep 4:1–2. 10.1179/135100099101534675

Figures

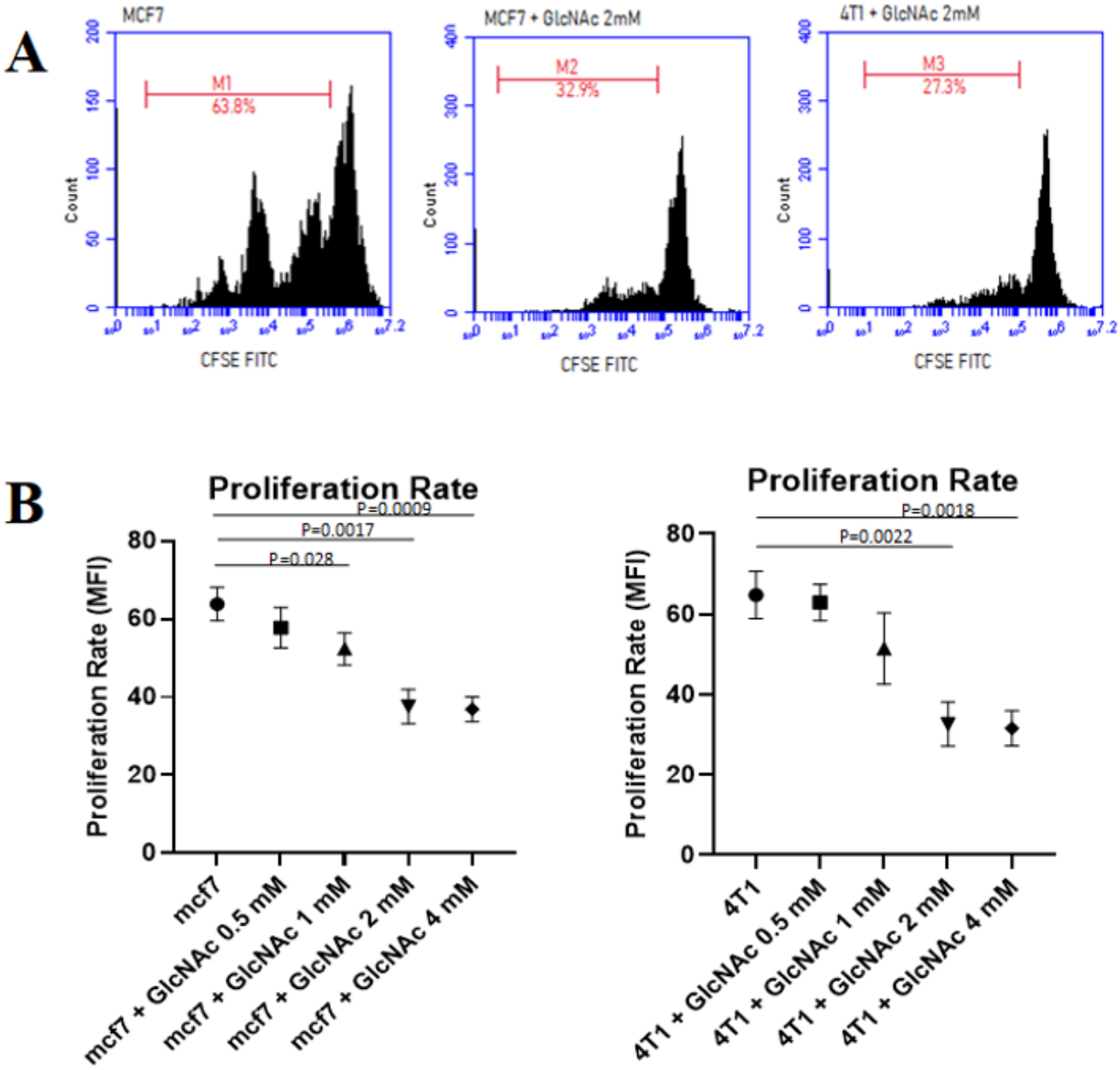

Figure 1

The proliferation rate of MCF-7 and 4T1 cells. **A,**The flow cytometry histogram analysis of MCF-7 and 4T1 cells in the presence and absence of D-GlcNAc. **B,** The statistical analysis of MCF-7 and 4T1 cells in the presence and absence of D-GlcNAc. 1 mM, 2 mM, and 4 mM D-GlcNAc significantly reduced the proliferation rate in MCF-7 cells, and 2 mM and 4 mM D-GlcNAc significantly reduced the proliferation rate in 4T1 cells (P<0.01-P <0.0001).

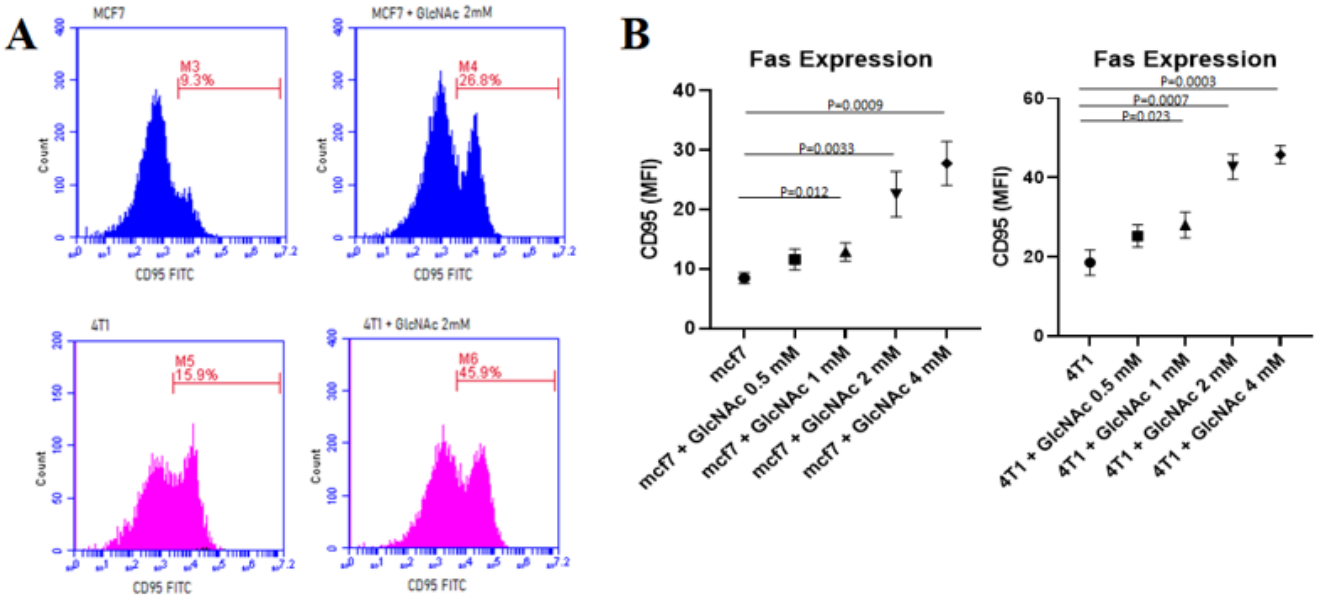

Figure 2

Fas expression on MCF-7 and 4T1 cells. **A,** The flow cytometry histogram analysis of MCF-7 and 4T1 cells in the presence and absence of D-GlcNAc. **B,** The bar graph shows the statistical analysis. 1 mM, 2 mM, and 4 mM D-GlcNAc significantly increased the Fas expression on MCF-7 and 4T1 cells (*P* <0.01-*P* <0.0001).

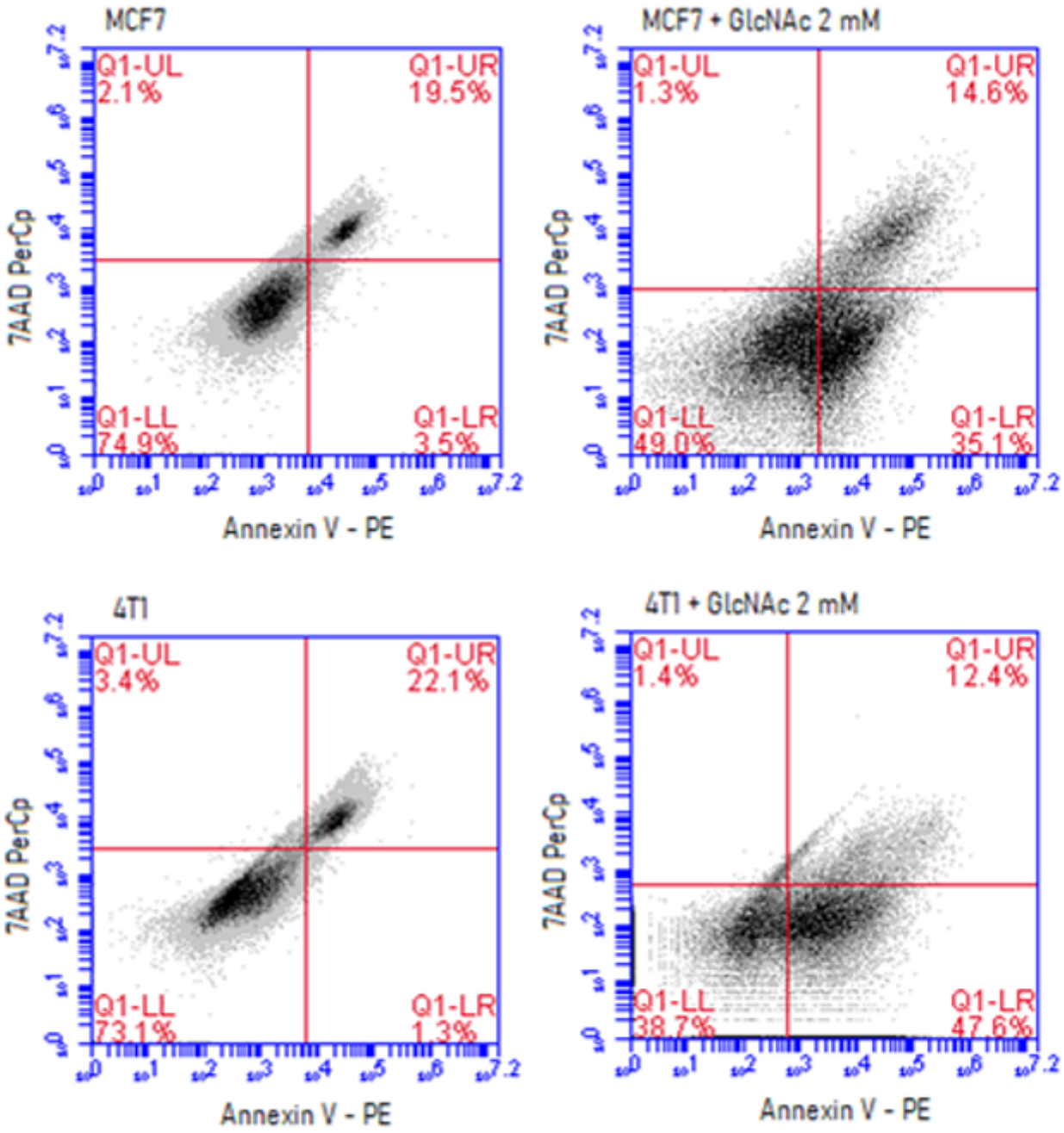

Figure 3

The flow cytometry dot-plot analysis of MCF-7 and 4T1 cells. Early apoptosis (bottom-right quadrant) increased in both MCF-7 and 4T1 cells in 2mM D-GlcNAc. The quadrants are as follows: **Top-right:** Late apoptosis. **Top-left:** Necrosis. **Bottom-right:** early apoptosis. **Bottom-left:**Living cells. Total apoptotic cells were calculated by subtracting the percentage of viable cells from the whole cells.

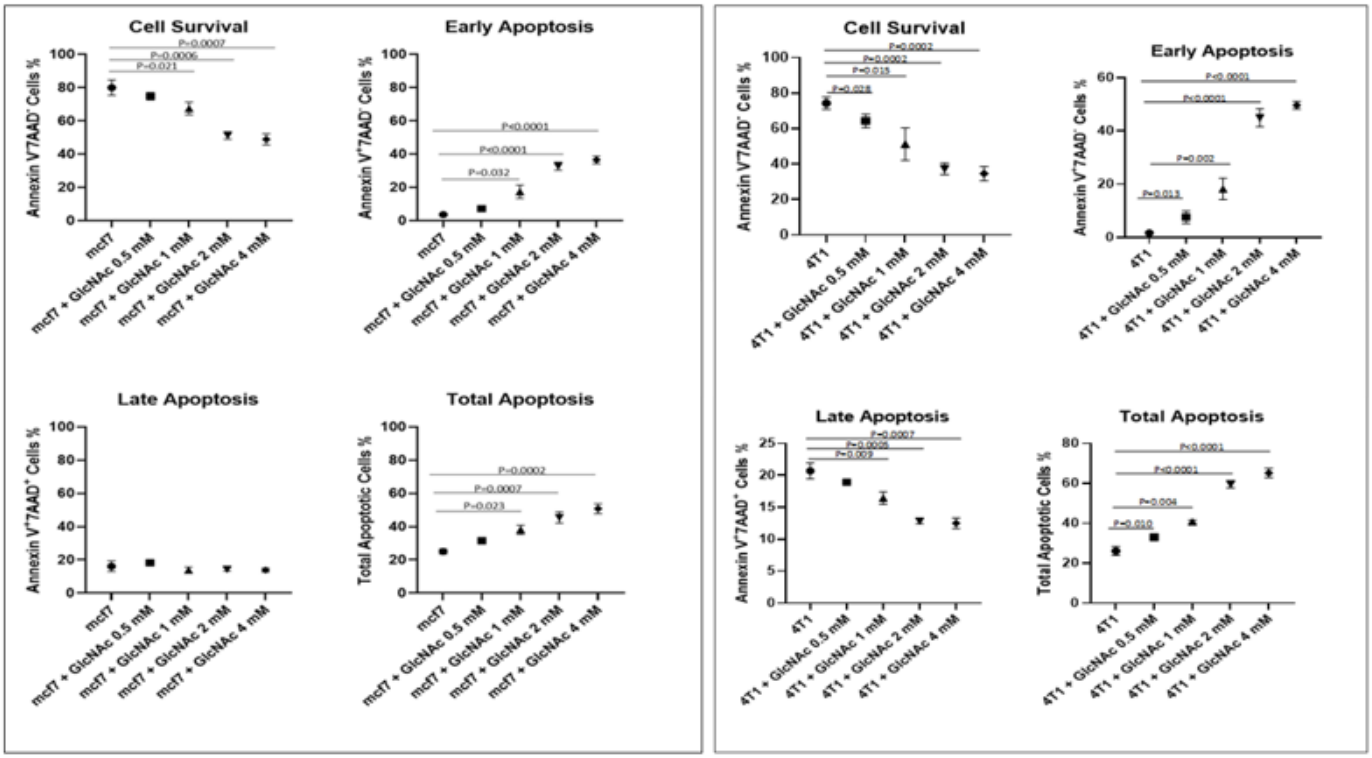

Figure 4

Statistical analysis of apoptosis observed on MCF-7 (left) and 4T1 (right) cells. Viable cells in MCF-7 and 4T1 cells with the presence of 1 mM, 2 mM and 4 mM D-GlcNAc were significantly reduced due to dose-dependent increases in the early apoptosis.

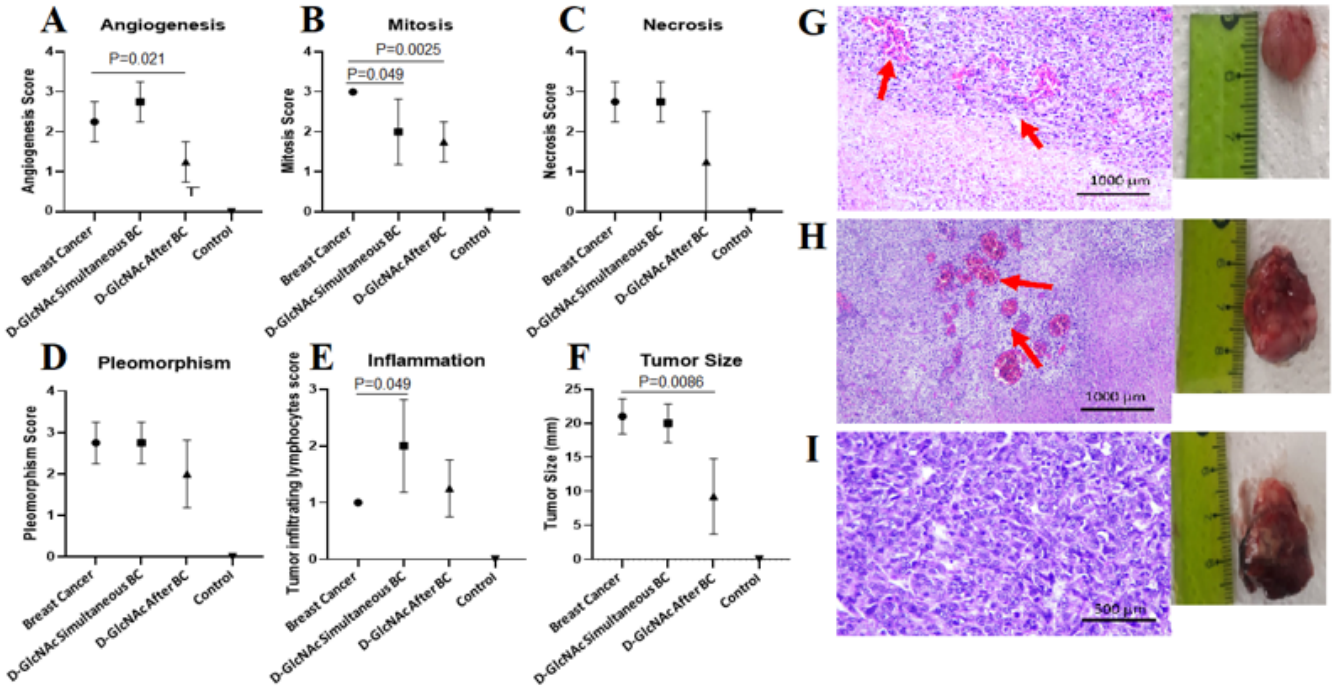

Figure 5

Tumour pathology and statistical analysis of breast tissues in the murine 4T1 model. **A,** angiogenesis was significantly reduced by D-GlcNAc in the post-treatment group. **B,** mitosis was significantly reduced by D-GlcNAc both in the pre-treatment and post-treatment groups. **C,** Necrosis tended to decrease in the post-treatment group. Still, the significant difference was not proved statistically due to the high standard deviation, compared with the breast cancer (BC) group, even though the mean value was less. **D,** Pleomorphism was not significantly changed with D-GlcNAc administration in pre-treatment or post-treatment groups due to high standard deviation. Still, the mean values of the post-treatment groups were less than the breast cancer group. **E,**The tumour-infiltrating cells significantly increased in the pre-treatment D-GlcNAc applied group compared with the breast cancer group. **F,** The tumor size significantly reduced in the post-treatment group compared with the breast cancer group. **G,** pre-treatment D-GlcNAc administration during tumor development; significant Necrosis, angiogenesis, and inflammation have shown with red arrows (10X magnification). **H,** D-GlcNAc treatment after tumour development; marked Necrosis and inflammation, low Pleomorphism, and low angiogenesis have shown with red arrows (10X magnification). **I,**Breast cancer without treatment; marked Pleomorphism and high mitosis observed in the breast tumor tissue (20X magnification).

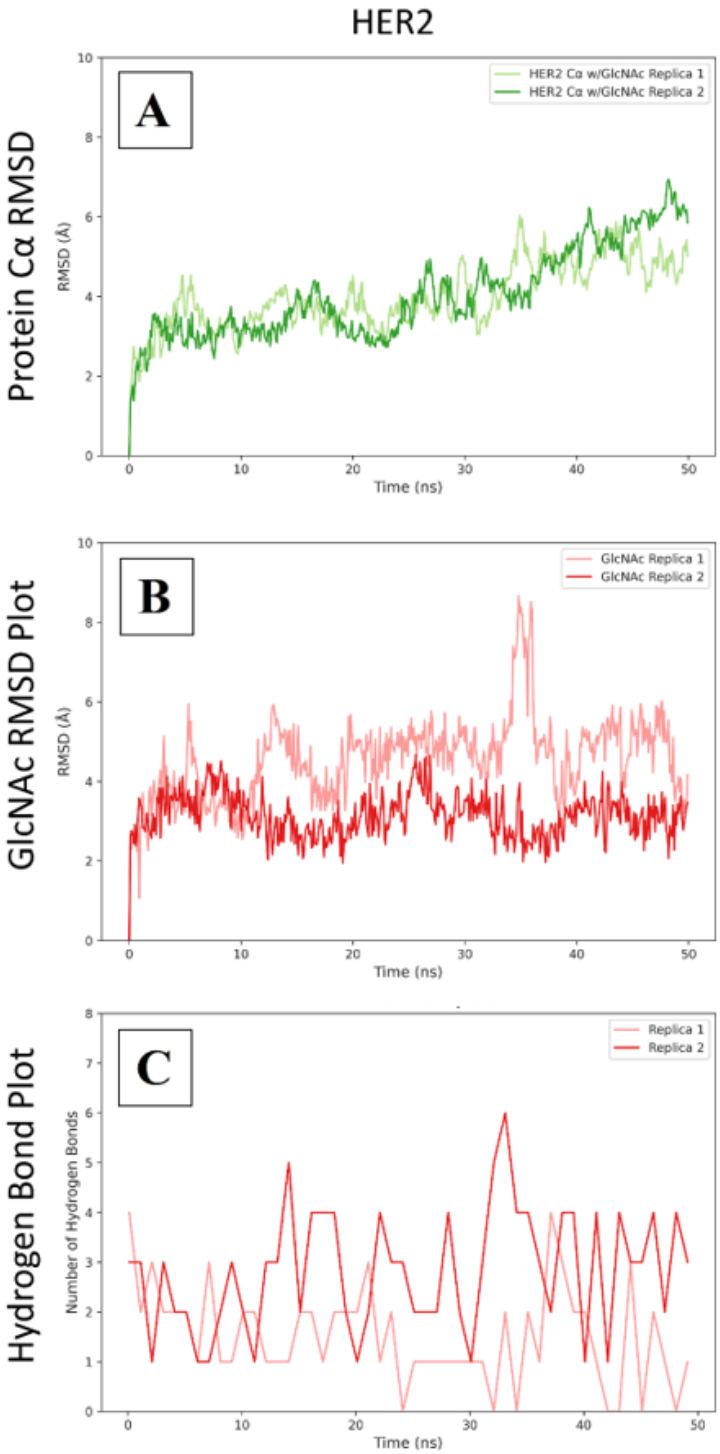

Figure 6

Molecular dynamics analysis plots. **A,** The Cα RMSD for the protein simulation over time. **B,** The RMSD of D-GlcNAc with each protein over time. **C,** The hydrogen bonds between the proteins and D-GlcNAc within 4 Å proximity over time. The column represents the plots of HER2. All experiments were performed in independent duplicates (replica 1 and replica 2 in the Figure).

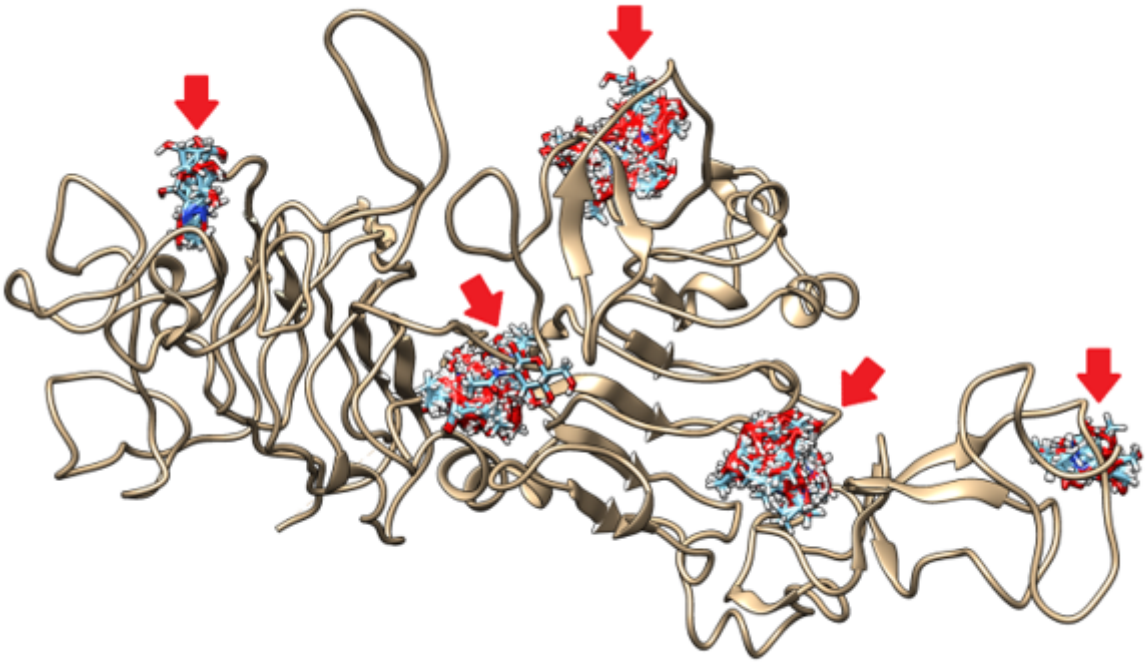

Figure 7

AutoDock results on HER2 and D-GlcNAc binding possibilities were confirmed by the SwissDock server. Red arrows show n-molecule binding ligands on different parts of the target protein.

Supplementary Files

This is a list of supplementary files associated with this preprint. Click to download.

- S1MCF7EC50Dataset.xlsx
- S2DockingSetting.txt
- S3MDSimulationConfiguration.txt
- S4MCF7EC50MLResults.xlsx
- S5ReproduceResults.py
- S6Noncovalentinteractions.txt
- S73WSQ.mpg